Seasonal changes in mesozooplankton swimmers collected by sediment trap moored at a single station of Northwind Abyssal Plain in the western Arctic Ocean

KOHEI MATSUNO[1]*, ATSUSHI YAMAGUCHI[2], AMANE FUJIWARA[1], JONAOTARO ONODERA[3], EIJI WATANABE[3], ICHIRO IMAI[2], SANAE CHIBA[3], NAOMI HARADA[3] AND TAKASHI KIKUCHI[3]

[1]ARCTIC ENVIRONMENT RESEARCH CENTER, NATIONAL INSTITUTE OF POLAR RESEARCH, 10-3 MIDORI-CHO, TACHIKAWA, TOKYO 190-8518, JAPAN,
[2]LABORATORY OF MARINE BIOLOGY, GRADUATE SCHOOL OF FISHERIES SCIENCES, HOKKAIDO UNIVERSITY, 3-1-1 MINATO-CHO, HAKODATE, HOKKAIDO 041-8611, JAPAN,
[3]JAPAN AGENCY FOR MARINE-EARTH SCIENCE AND TECHNOLOGY, NATSUSHIMA-CHO 2-15, YOKOSUKA, KANAGAWA 237-0061, JAPAN

* CORRESPONDING AUTHOR: matsuno.kohei@nipr.ac.jp, k.matsuno@fish.hokudai.ac.jp

KEYWORDS: copepods; life cycle; Pacific water; sea ice; sediment trap

RUNNING HEAD: Seasonal changes of mesozooplankton in Arctic Ocean

Abstract

To examine seasonal changes in mesozooplankton community, analyses were made on the swimmer samples (>1 mm) collected by a sediment trap mooring at 184 m depth of Northwind Abyssal Plain in the western Arctic Ocean during October 2010 to September 2011. The zooplankton swimmer flux ranged 5−44 ind. m^{-2} day^{-1} and was greater during July to October; copepods were the dominant taxon. Based on the zooplankton swimmer flux, cluster analysis classified samples into three groups (A, B-1 and B-2). The occurrence of each group showed clear seasonality; group A was observed during July to October, group B-1 was seen in November to January, and group B-2 was seen during March to June. The seasonal variability in population structures of four dominant copepod swimmers were clearly different among the species. Most *Calanus hyperboreus* were C6F throughout the year. For *Metridia longa* and *Paraeuchaeta glacialis*, C6Fs dominated during January to May, and early copepodid stages increased during June to October. *Heterorhabdus norvegicus* was dominated by C5 during November to February, and C6F/M during March to May. Since Pacific copepods (*Neocalanus cristatus*) occurred with significant number during August−September, possible causes are discussed.

INTRODUCTION

After 1990's, a drastic reduction of sea ice cover area has been observed in the Arctic Ocean during summer (July−October). This reduction is considered to have been caused by an increased flow of warm Pacific Summer Water (PSW) from the Bering Sea Strait into the Arctic Ocean (Shimada *et al.*, 2006; Woodgate *et al.*, 2010). The Pacific sector of the Arctic Ocean comprises both shallow (Chukchi Sea and East Siberian Sea) and deep (Canada Basin and Mendeleyev Ridge) areas (Fig. 1). Sea ice reduction in this region has been the greatest in the Arctic Ocean (Shimada *et al.*, 2001, 2006; Stroeve *et al.*, 2007; Comiso *et al.*, 2008; Markus *et al.*, 2009), and this reduction of sea ice is expected to alter the marine ecosystem structure in the Arctic Ocean (Grebmeier *et al.*, 2006; Hunt and Drinkwater, 2007; Grebmeier, 2012).

The zooplankton community in the western Arctic Ocean has been studied based on net

samples (Springer *et al.*, 1989; Darnis *et al.*, 2008; Hopcroft *et al.*, 2010; Matsuno *et al.*, 2011, 2012). However, seasonal sea ice coverage in this area prevents collection of net samples in winter, and most of the studies were conducted only in summer. To evaluate seasonal changes in zooplankton community, analysis on zooplankton swimmers (Knauer *et al.*, 1979) collected by moored sediment trap is a powerful tool (cf. Forbes *et al.*, 1992). According to Knauer *et al.* 1979, swimmer is defined that zooplankton actively swam into the trap and was killed by the preservation fluid filled with the cups. Because of their importance, seasonal changes in swimmer community collected by sediment trap have been studied in several areas of the Arctic Ocean, especially in the Beaufort Sea (Forbes *et al.*, 1992; Ota *et al.*, 2008; Makabe *et al.*, 2010). According to Makabe *et al.* (2010), seasonal changes in Arctic swimmer community are related to the sea ice concentration, temperature and salinity. This is partly because large copepods migrate to surface when the sea ice melts (Conover and Huntley, 1991), graze on phytoplankton in the ice-edge bloom (Springer and McRoy, 1993), and then reproduce. The reproduction seasons of dominant copepods vary with species and areas within the Arctic Ocean (Falk-Petersen *et al.*, 2009). Despite their importance, little information is available for life cycle of copepods other than dominant species. For dominant copepods, their species-specific lipid accumulation and gonad maturation have little evaluated in the western Arctic Ocean.

In the present study, we analyzed zooplankton swimmers collected by sediment trap sampling at 13−15 day intervals moored at 184 m in Northwind Abyssal Plain during October 2010 to September 2011. Through this analysis, seasonal changes in swimmer community structure and population structure of the four dominant copepods (*Calanus hyperboreus*, *Metridia longa*, *Paraeuchaeta glacialis* and *Heterorhabdus norvegicus*) were evaluated. Lipid accumulation and gonad maturation of adult females (C6F) from the dominant copepods were analyzed to evaluate their life cycle patterns. Seasonal occurrence of the Pacific copepods (*Neocalanus cristatus*) was also noted and the possible cause was discussed.

METHOD

Field sampling

Samples were collected by sediment trap (SMD26 S-6000, open mouth area 0.5 m^2, Nichiyu Giken Kogyo, Co. Ltd.) rotated at 13−15 day intervals moored at 184 m and 1,300 m at St. NAPt (Northwind Abyssal Plain trap, 75°00´N, 162°00´W, bottom depth 1975 m) during 4 October 2010 to 28 September 2011 (Fig. 1). This station is seasonally affected by inflow of Bering Shelf Water (BSW) from Bering Strait (Weingartner *et al.*, 2005; Woodgate *et al.*, 2005). The end of the trap rope was fixed to the sea bottom. Sea water for filling sample cups was taken from 1,000 m water depth in the southern Canada Basin (salinity 34.89), and was filtered with membrane filter (0.45 µm pore size) to make 5% buffered formalin seawater. The sample cups were filled with the 5% buffered formalin seawater before the sediment trap was deployed.

After the trap was retrieved, the 26 samples each were gently filtered with 1 mm mesh, and the remaining fraction (>1 mm size) on the mesh was treated as zooplankton swimmers. Since the number of zooplankton swimmer was low for deeper trap (1,300 m), we treated only shallower trap (184 m) in this study. The fine size fraction (<1 mm) for each sample was evenly divided to 10 aliquots using the Wet Sample Divider (McLane™ WSD-10). The one of divided aliquots for each sample was filtered on weighed polycarbonate membrane filter, and was desalted with Milli-Q waters. The sample filters were dried with diphosphorus pentaoxide in desiccator for three days. The dried sample filters were weighed with analytical balance to calculate total mass flux (mg dry mass [DM] m^{-2} day^{-1}) of < 1 mm size fraction for each sample period.

As the supplemental environmental data, the moored trap depth and the water temperature (accuracy of ±0.2°C) were monitored every hour (sensor type: ST-26S-T). We estimated the current speed at St. NAPt in 2010 by a physical ocean general circulation model: Center for Climate System Research Ocean Component Model (COCO) version 4.9. The model performance in the western Arctic Ocean has been verified in previous decadal and seasonal experiments (Watanabe *et al.*, 2012; Watanabe and Ogi, 2013). Time-series data on weekly averaged percentage ice coverage around St. NAPt (74.5−75.5°N, 161.5−162.5°W) during the mooring period were calculated from the sea ice concentration data set (http://iridl.ldeo.columbia.edu/SOURCES/.IGOS-

S/.nmc/.Reyn_SmithOIv2/, cf. Reynolds *et al.*, 2002). For sea ice coverage data of whole Arctic Ocean, the data were downloaded from the AMSER-E data set (http://www.ijis.iarc.uaf.edu/seaice/-extent/plot.csv). The MODIS/Aqua Level 3 binned chlorophyll-*a* data (reprocessing version 2012.0) were downloaded from the Distributed Active Archive Center (DAAC) of Goddard Space Flight Center (GSFC), NASA. We used daily data at 9-km resolution, and composited to 9 days running mean.

Analysis of zooplankton swimmer

For zooplankton swimmer samples (>1 mm), identification and enumeration of zooplankton were made under a dissecting microscope. In this study, swimmer defined that zooplankton in >1 mm samples swam actively into the trap (cf. Knauer *et al.*, 1979). Specimens damaged before collection were distinguished based on the description of Sampei *et al.* (2009), while their contribution was small (<0.65% in total count) and excluded from following analysis. Species identification of copepods followed mainly Brodsky (1967) and Frost (1989) for *Pseudocalanus* spp. (*P. minutus* and *P. newmani*), Frost (1974) for *Calanus* spp. (*C. glacialis* and *Calanus marshallae*), and Miller (1988) for *Neocalanus* spp. Identification of the four dominant calanoid copepods (*Calanus hyperboreus*, *Metridia longa*, *Paraeuchaeta glacialis* and *Heterorhabdus norvegicus*) was made to the copepodid stage level.

For *C. hyperboreus*, *M. longa* and *P. glacialis*, the copepodid stage 6 females (C6Fs) contain a large oil sac in the prosome. To analyze the amount of oil, oil length relative to prosome length (PL) was scored into three groups: I (the lipid length is 0−4% of PL), II (4−40% of PL) and III (>40% of PL). For the same three species, gonad maturation of the C6F was also scored into three groups: I (immature), II (small oocytes in ovary or oviduct) and III (large eggs or distended opaque in oviduct). For this gonad maturation index, we referred to those used previously for *C. hyperboreus* (Hirche and Niehoff, 1996) and *M. longa* (Tande and Grønvik, 1983). Of the four dominant copepods, only *H. norvegicus* was not analyzed for lipid accumulation and gonad maturation, because of the difficulty in observation. *Heterorhabdus norvegicus* accumulate lipids

in many small oil droplets, and the low transparency of the prosome prevents observation of their gonad.

The flux (F, ind. m^{-2} day^{-1}) of zooplankton swimmers was calculated from the following equation:

$$F = N \times \frac{1}{0.5} \times \frac{1}{d}$$

where N is the number of individuals (ind.), 0.5 is the mouth area (m^2) of the sediment trap, and d is the sampling interval (days). We counted total zooplankton swimmers 37−288 individuals per sample. Since the sampling interval is similar (13−15 days) throughout the sampling period, conversion factor between count and flux was similar (one individual $sample^{-1}$ corresponded to 0.133−0.154 ind. m^{-2} day^{-1} [=1/0.5/13−15]).

Data analysis

Zooplankton swimmer flux data (F: ind. m^{-2} day^{-1}) for each species was log transformed ($\log_{10}[X+1]$) prior to analysis to reduce the bias of flux. Similarities between samples were examined using the Bray-Curtis index (Bray and Curtis, 1957). To group samples, the similarity indices were coupled with hierarchical agglomerative clustering using a complete linkage method (Unweighted Pair Group Method using Arithmetic mean: UPGMA) (Field *et al.*, 1982). All of these analyses were carried out using PRIMER v6 software (PRIMER-E Ltd.). Inter-group differences in flux of all zooplankton swimmers were tested by one-way ANOVA and an ex post facto test by Fisher's Protected Least Significant Difference test (PLSD). These statistical analyses were carried out using StatView v5 software (SAS Institute Inc.).

RESULTS

Hydrography

The trap depth varied between 181 and 218 m (Fig. 2a), and was stable around 184 m most of the date then temporally deepened (220 m) within short period (6−7 days) in October, December 2010

and September 2011. Temperature at sediment trap ranged from −1.6 to −0.6°C (Fig. 2b). Rapid decreases in temperature were paralleled with the deepening changes in the moored trap depth (Fig 2a, b). The five days mean of current velocity simulated by ocean circulation model showed slow subsurface current (<11.3 cm s^{-1} at 45 m and <2.7 cm s^{-1} at 188 m water depths) at St. NAPt (Fig. 2c). From two times CTD casts at the station, four water masses were identified at 0−500 m water column: i.e. SML: Surface Mixed Layer (0−25 m), PSW: Pacific Summer Water (25−100 m), PWW: Pacific Winter Water (100−250 m), AW: Atlantic Water (>250 m) (Fig. 2d, e) (McLaughlin *et al.*, 2011).

Sea ice around the sediment-trap site showed clear seasonal changes, with a decrease from early July, complete melting (sea ice concentration: 0%) in September, a rapid increase during October, and 100% coverage during November to June (Fig. 3a). The total mass flux (<1 mm size range) ranged 19.3−215.9 mg DM m^{-2} day^{-1} and peaked during November−December (Fig. 3a). High chl. *a* was observed during August−September (Fig. 3a). At St. NAPt, the midnight sun occurred during early May to early August, and polar night was from early November to early February (Fig. 3b).

Swimmer community

Based on the zooplankton swimmer flux, cluster analysis classified the zooplankton swimmer communities largely (A and B) at 55% dissimilarity level, then group B subdivided (B-1 and B-2) at 47% dissimilarity level (Fig. 4a). Occurrence of each group showed distinct seasonality. Group A (n = 8) was observed from July to October, group B-1 (n = 6) from November to January, and group B-2 (n = 9) from March to June (Fig. 4b). Zooplankton swimmer flux ranged from 5 to 44 ind. m^{-2} day^{-1}. While except extremely high peak of amphipods (*Themisto libellula*) in April, zooplankton swimmer flux was highest during July to October (Fig. 4b). The averaged zooplankton swimmer flux was highest in A (20.0±4.9 ind. m^{-2} day^{-1}), lower in B-2 (16.1±3.9), and lowest in B-1 (11.9±2.4). Copepods comprised 18 to 94% of the zooplankton swimmer flux and were the dominant taxon; amphipods the second most dominant group (0−74%) (Fig. 4b). The

characterized species of each group (significantly abundant than the other groups analyzed by one-way ANOVA and Fisher's PLSD, $p<0.05$) were as follows: A, the mesopelagic copepods *Paraeuchaeta glacialis*; and B-2, the inter-zonal copepod *Calanus hyperboreus*. While group B-1 dominated by *Metridia longa* and *Heterorhabdus norvegicus*, their flux showed no significant seasonal changes.

Copepod population structure

The population structures of the four dominant copepods (*C. hyperboreus*, *M. longa*, *P. glacialis* and *H. norvegicus*) varied with species. Throughout the year, *C. hyperboreus* was predominated by C6F (Fig. 5a). The population structure of *M. longa* and *P. glacialis* showed seasonal change; both were dominated by C6F from January to May, and early copepodid stages (C1−C4) occurred during June−October (Fig. 5b, c). *Heterorhabdus norvegicus* showed a different seasonal pattern; it was dominated by C5 during November−February, the contribution of C6F/M increased during March−October, and C1 and C2 stages occurred in June−July (Fig. 5d).

Lipid accumulation in C6Fs of the dominant copepods (excluding *H. norvegicus*) also showed species-specific seasonal patterns. Most *C. hyperboreus* contained more lipids (stage III) during December−January (83%) than during February−October (56%) (Fig. 6a). For *M. longa*, stage III individuals dominated during October−December, their composition gradually decreased during March to June, and all specimens had no oil sacs in July (Fig. 6b). The lipid accumulation of *P. glacialis* showed fluctuated seasonal change (Fig. 6c).

Gonad maturation of C6Fs of the dominant copepods (excluding *H. norvegicus*) showed more distinct seasonality. For *C. hyperboreus*, mature individuals were observed only during February−April (Fig. 6d). Mature *M. longa* were seen during March−July, note that in September was based on only one specimen (Fig. 6e), with the lipid accumulation decreased (Fig. 6b). Most *P. glacialis* (47%) matured during August−January (Fig. 6f), when egg carrying *P. glacialis* C6Fs were also seen.

Pacific copepods

The Pacific copepod *Neocalanus cristatus* occurred (0−0.92 ind. m^{-2} day^{-1}) throughout the year, and was higher during August−September when the sea ice was reduced (Fig. 7). All *N. cristatus* were stage C5, and lipid accumulation varied.

DISCUSSION

Trap collection efficiency

In general, underestimate bias in sinking particle flux is concerned due to low trap collection efficiency under flowing water condition especially shallower than 1,000 m (Buesseler *et al.*, 2007). The time-series monitoring data for physical oceanography around St. NAPt are limited. However, the directly measured water current around St. NAPt in winter was slower than 10 cm s^{-1} at 58 and 250 m water depths (Sumata and Shimada, 2007). The current speed estimated by ocean circulation model also confirmed that the speed of the subsurface current around trap was slow (<2.7 cm s^{-1}) at St. NAPt throughout the year (Fig. 2c). These slow current speeds were not expected to have a significant effect on sediment trap collection efficiency. The sediment trap temporarily deepened to 220 m with short period (6−7 days) in October, December 2010 and September 2011 (Fig. 2a). Temporal changes in temperature also confirmed these changes (Fig. 2b). The tilt of sediment trap was estimated within 15° in the deepening events. Except for these periods, mooring depth of sediment trap was kept 180−190 m. Since the PWW were occurred between 100−250 m (Fig. 2d, e), there expected little changes in water masses at the trap depth. Although the deployment depth of sediment trap was not completely constant throughout the studied period, the seasonality of total mass fluxes at 184 m trap and at 1,300 m trap (Onodera *et al.*, pers. comm.) was well paralleled (r^2 = 0.621, p<0.0001). These results suggest that the influence of the trapping efficiency bias is usually insignificant for the studied sediment trap samples.

Seasonal changes in swimmer community

Previously reported zooplankton swimmer communities collected by sediment trap in the Arctic

Ocean are summarized in Table 1. Throughout the studies, copepods are the most dominant taxa, followed by amphipods or pteropods similar with this study. Within the copepods, *C. finmarchicus* is reported to be dominated for the shallower trap (ca. 100 m) in the Norwegian fjord faced to the North Atlantic Ocean (Willis *et al.*, 2006, 2008). While in the deep-layer (500 m) of the eastern Greenland Sea, *C. finmarchicus* was lesser and dominated by *M. longa* (Seiler and Brandt, 1997). For the western Arctic Ocean (Amundsen Gulf and Beaufort Sea), not faced to the Atlantic Ocean, *C. finmarchicus* did not occur and *M. longa* was dominated (Forbes *et al.*, 1992; Sampei *et al.*, 2012). For the northernmost station (81°N), diapausing *C. hyperboreus* was predominated (Hargrave *et al.*, 1989). Thus, the dominant copepod species collected by sediment trap may vary with region and trap depths. The trap depth of this study (184 m) was relatively shallow, but because the NAPt is not faced to the Atlantic Ocean, *C. finmarchicus* did not occur. Dominant copepods of this study, *H. norvegicus* followed with *M. longa*, were a unique, because of the dominance of the mesopelagic copepods (Yamaguchi and Ikeda, 2000). *Heterorhabdus norvegicus* is reported to be the second dominant copepods in the zooplankton swimmer fauna of the eastern Greenland Sea (Seiler and Brandt, 1997), thus this species may be dominant copepods throughout the mesopelagic layer of the Arctic Ocean. Copepod fauna evaluated by stratified net samplings also noted the occurrence of *H. norvegicus* throughout the Arctic Ocean (Kosobokova and Hirche, 2000; Auel and Hagen, 2002; Kosobokova and Hopcroft, 2010; Dvoretsky and Dvoretsky 2011). Add to these copepods, occurrence of small number of the Pacific copepods is a special feature of this study. Since the zooplankton swimmer community of this study showed clear seasonal changes (groups A, B-1 and B-2), following, we discuss the characteristics of each swimmer group.

The group A, corresponded with open water period (July−October), dominated by the carnivorous *P. glacialis* (3.7−9.4 times greater flux than the other groups, one-way ANOVA, $p<0.001$). For the numerical dominance of *P. glacialis* during July−October, two factors are considered: i) correspondence of growth to large copepodid stages (>1 mm in size), ii) correspondence of presence of massive diel vertical migration (DVM) at that period. For the

former, dominance of C5 stage during the period (Fig. 5c) suggests that the major population grew up this season. For the latter, *P. norvegica*, which is an Atlantic congener species for *P. glacialis*, is known to perform DVM during autumn (Kaartvedt *et al.*, 2002), but cease DVM during midnight sun and polar night (Fleddum *et al.*, 2001). At St. NAPt, the midnight sun occurred during early May to early August, and polar night was from early November to early February (Fig. 3c). Thus, if *P. glacialis* had similar DVM of *P. norvegica*, the dominance of *P. glacialis* in group A (July−October) was caused by the presence of DVM for *P. glacialis* during that period.

Changes in zooplankton swimmer community from group A to B-1 was corresponded with the timing of ice coverage and entered polar night (Fig. 3c). The group B-1 was characterized with the dominance of mesopelagic *M. longa* and *H. norvegicus*. While their flux showed little seasonal changes (Fig. 5b, d), the other two species showed clear seasonality: peaked in May−June for *C. hyperboreus* (Fig. 5a) and July−October for *P. glacialis* (Fig. 5c). Thus, group B-1 was composed mainly by mesopelagic copepods (*M. longa* and *H. norvegicus*) stable occurred in the mesopelagic layer. For the other two species (*C. hyperboreus* and *P. glacialis*), seasonal vertical migration (SVM) and presence/absence of DVM is considered to be a key mechanism to govern the seasonal changes in swimmer community.

During the ice coverage period (November−June), the swimmer community changed from group B-1 to B-2 in February due to the drastic increase (ca. 10 times) of *C. hyperboreus* (one-way ANOVA, $p<0.01$). *Calanus hyperboreus* is known to perform SVM (Hirche, 1997; Vinogradov, 1997), diapause at depth (500−1,500 m) in winter, and make upward SVM to the surface layer in April (Hirche and Niehoff, 1996). In the present study, it was shown that *C. hyperboreus* included only C6Fs and their flux increased from February and peaked in May (Fig. 5a). This increase in flux during February to May was presumably due to their upward SVM from deep layer. Therefore, the change in swimmer community (from group B-1 to B-2) during January−March might have been caused by the upward SVM of *C. hyperboreus*. For arousal mechanism of resting copepods, presence of an internal body timer is discussed (Miller and Grigg, 1991; Miller *et al.*, 1991). Since daylight hours changed greatly from zero (polar night) to 24h (midnight sun) during

February to April (Fig. 3c), this change in day-night cycle may affect the arousal of diapause for *C. hyperboreus*.

As specialized seasonal event of this study, the occurrence of Pacific copepods was observed. The Pacific copepod *N. cristatus* C5 was abundant during August−September when sea ice coverage decreased (Fig. 8). This seasonal pattern suggests that the amount of the inflow Pacific Water may increase when the sea ice coverage decreases. While *N. cristatus* C5 is known to perform SVM to deep layer to diapause during late summer (Miller *et al.*, 1984), the greater flux of *N. cristatus* C5 in August−September may also be caused by their SVM. Since their reproduction occurs >1,000 m depth (Miller *et al.*, 1984), the possibility of their reproduction in the Arctic Ocean could not be evaluated from this study.

Population structure of dominant copepods

Calanus hyperboreus populations were composed much of C6F throughout the year (Fig. 5a). *Calanus hyperboreus* reproduces during November−April in Amundsen Gulf (Ota *et al.*, 2008), November−March in the Greenland Sea (Hirche and Niehoff, 1996), and February−March in the Norwegian Sea (Østvedt, 1955). In the present study, mature C6F were seen only from February to April, which suggests this is the reproduction period (Fig. 8). This reproduction season (February−April) generally corresponds to the previous studies with slight seasonal variances. For the regional variability in reproduction timing of *C. hyperboreus*, timing of the phytoplankton bloom is reported to be a most important factor (Conover and Siferd, 1993; Hirche and Niehoff, 1996). Full-lipid individuals in stage C6F dominated in December−January, and the lipid accumulation decreased from February when the reproduction started (Fig. 6a). This seasonal correspondence between reproduction period and decrease of lipid accumulation would be caused by the utilization of the stored lipid to reproduction (Hirche and Niehoff, 1996; Vinogradov, 1997).

The *M. longa* population was dominated by C6F during January−May, and early copepodid stages (C1−C4) during June−October (Fig. 5b). *Metridia longa* is omnivore and performs diel vertical migration (Conover and Huntley, 1991; Ashjian *et al.*, 1995), and has no diapause phase

(Båmstedt and Ervik, 1984; Grønvik and Hopkins, 1984). The main reproduction season shows regional variability: during April−May in the Balsfjorden (Tande and Grønvik, 1983), in winter under the sea ice in the Barents Sea (Hirche and Kosobokova, 2011), and in autumn in a polynya in the Beaufort Sea (Makabe *et al.*, 2010). In this study, mature C6F occurred only during March−July (Fig. 6e), and early copepodid stages (C1−C4) dominated the population during June−October (Fig. 5b). These facts suggest that *M. longa* reproduces during March−July and the new population appear during June−October. This reproduction season (March−July) in the western Arctic Ocean is slightly longer than that in the Balsfjorden (April−May) (Tande and Grønvik, 1983). Lipid accumulated (stage III) individuals dominated during October−December, decreased gradually over winter and no specimens had oil sacs in July (Fig. 6b). This season of decreasing lipids (March−June) parallels the gonad maturation season (March−July). These facts suggest that the stored lipids are used for gonad maturation of *M. longa* as was seen in *C. hyperboreus*.

The *P. glacialis* population was dominated by C6F during January−May, and contained early copepodid stages (C2−C4) during June−October (Fig. 5c). Carnivorous *Paraeuchaeta* spp. performs raptorial feeding throughout the year, accumulate much lipids, and have no diapause phase (Båmstedt, 1979; Øresland, 1991). Since mature C6F *P. glacialis* dominated during August−January and egg carrying C6F also occurred during the same period (Fig. 6f), this species is assumed to reproduce in this period. This may be related to the ice-edge bloom at the surface. Ice-edge bloom is known to be occurred after ice melting (Springer and McRoy, 1993) (Fig. 3b). Ice-edge bloom induces the upward migration of Arctic copepods (e.g., *C. glacialis*) and reproduction of small copepods (e.g., *Pseudocalanus* spp.) (Conover and Huntley, 1991), which would provide sufficient food condition for carnivorous *P. glacialis*. Since sufficient food condition (abundant small metazoan zooplankton) is a key to make growth and reproduction of *Paraeuchaeta* spp. (Yamaguchi and Ikeda, 2001; Abe *et al.*, 2012), *P. glacialis* may have performed reproduction in this season. This reproduction season of *P. glacialis* (August−January) differs with those of *C. hyperboreus* (February−April) and *M. longa* (March−July). These differences

may be related to differences in feeding modes, i.e., carnivory in *P. glacialis* and suspension feeding in *C. hyperboreus* and *M. longa*.

The *H. norvegicus* population was dominated by C5 during November−February and C6F/M during March−October, and C1 and C2 were collected in June and July (Fig. 5d). Since lipid accumulation and gonad maturation could not be analyzed for *H. norvegicus*, the reproduction season was estimated from the population structure data. Combining dominance of early copepodid stage (June and July) and assuming development time of *Heterorhabdus* spp. nauplii (1−2 months) (Yamaguchi and Ikeda, 2000), the reproduction season is thought to be during April and May. Little comparable information is available for the life cycle of *H. norvegicus*. Thus, the reproduction seasons of the dominant four copepods differed (Fig. 8), and possible causes of these differences include species-specific feeding modes, seasonal changes in food availability, and the presence/absence of ontogenetic vertical migration.

In summary, while the limitation of sampling design (data based on single sediment trap at a single station and depth), through the analyses on zooplankton swimmers collected by a sediment trap, zooplankton communities were clearly separated into three seasons (Fig. 8). The season when each copepod dominated corresponded with the reproduction timing of each species. For the four dominant copepods, their reproduction timings varied with species, which may be related to the feeding modes. In addition, the occurrence of the Pacific copepods was observed. Since their peak period (August−September) corresponded with timing of their SVM, they may enter sediment trap to perform descent SVM.

ACKNOWLEDGEMENTS

We are grateful to the captain, officers and crews of the R.V. Mirai (JAMSTEC), operated by GODI, R/V CCGS Sir Wilfrid Laurier, and Dr. Humfrey Melling (IOS, Canada) for their help in the mooring operation and sampling collection. We thank Dr. John Richard Bower (Hokkaido University) for correcting English of this manuscript. Drs. Yasunori Sakurai, Kenshi Kuma and Toru Hirawake (Hokkaido University) provided valuable comments on an earlier draft of the

manuscript.

FUNDING

This study was supported by Green Network of Excellence Program (GRENE Program), Arctic Climate Change Research Project ‘Rapid Change of the Arctic Climate System and its Global Influences’ and Grant-in-Aid for Scientific Research (S) 22221003 Catastrophic reduction of sea-ice in the Arctic Ocean −its impact on the marine ecosystems in the polar region− to NH and JSPS Fellows (234167) to KM. Part of this study was supported by Grant-in-Aid for Scientific Research (A) 24248032 and Grant-in-Aid for Scientific Research on Innovative Areas 24110005 from the JSPS.

REFERENCES

Abe, Y., Ishii, K., Yamaguchi, A. *et al.* (2012) Short-term changes in population structure and vertical distribution of mesopelagic copepods during the spring phytoplankton bloom in the Oyashio region. *Deep-Sea Res. I*, **65**, 100−112.

Ashjian, C.J., Smith, S.L. and Lane, P.V.Z. (1995) The Northeast Water Polynya during summer 1992: distribution and aspects of secondary production of copepods. *J. Geophys. Res.*, **100**, 4371−4388.

Auel, H. and Hagen, W. (2002) Mesozooplankton community structure, abundance and biomass in the central Arctic Ocean. *Mar. Biol.*, **140**, 1013−1021.

Båmstedt, U. (1979) Reproduction bioenergetics within the summer and winter generations of *Euchaeta norvegica* (Copepoda). *Mar. Biol.*, **54**, 135−142.

Båmstedt, U. and Ervik, A. (1984) Local variations in size and activity among *Calanus finmarchicus* and *Metridia longa* (Copepoda, Calanoida) overwintering on the west coast of Norway. *J. Plankton Res.*, **6**, 843−857.

Bray, J.B. and Curtis, J.T. (1957) An ordination of the upland forest communities of southern Wisconsin. *Ecol. Monogr.*, **27**, 325−349.

Brodsky, K.A. (1967) *Calanoida of the Far-eastern Seas and Polar Basin of the USSR*. Israel Program Scientific Translation, Jerusalem.

Buesseler, K.O., Antia, A.N., Chen, M. *et al.* (2007) An assessment of the use of sediment traps for estimating upper ocean particle fluxes. *J. Mar. Res.*, **65**, 345−416.

Comiso, J.C., Parkinson, C.L., Gersten, R. *et al.* (2008) Accelerated decline in the Arctic sea ice cover. *Geophys. Res. Lett.*, **35**, L01703, doi: 10.1029/2007GL031972.

Conover, R.J. and Huntley, M. (1991) Copepods in ice-covered seas−Distribution, adaptations to seasonally limited food, metabolism, growth patterns and life cycle strategies in polar seas. *J. Mar. Syst.*, **2**, 1−41.

Conover, R.J. and Siferd, T.D. (1993) Dark-season survival strategies of coastal zone zooplankton in the Canadian Arctic. *Arctic*, **46**, 303−311.

Darnis, G., Barber, D.G. and Fortier, L. (2008) Sea ice and the onshore−offshore gradient in pre-winter zooplankton assemblages in southeastern Beaufort Sea. *J. Mar. Syst.*, **74**, 994−1011.

Dvoretsky, V.G. and Dvoretsky, A.G. (2011) Copepod communities off Franz Josef Land (northern Barents Sea) in late summer of 2006 and 2007. *Polar Biol.*, **34**, 1231−1238.

Falk-Petersen, S., Mayzaud, P. and Kattner, G. (2009) Lipids and life strategy of Arctic *Calanus*. *Mar. Biol. Res.*, **5**, 18−39.

Field, J.G., Clarke, K.R. and Warwick, R.M. (1982) A practical strategy for analyzing multispecies distribution patterns. *Mar. Ecol. Prog. Ser.*, **8**, 37−52.

Fleddum, A., Kaartvedt, S. and Ellertsen, B. (2001) Distribution and feeding of the carnivorous copepod *Paraeuchaeta norvegica* in habitats of shallow prey assemblages and midnight sun. *Mar. Biol.*, **139**, 719−726.

Forbes, J.R., Macdonald, R.W., Carmack, E.C. *et al.* (1992) Zooplankton retained in sequential sediment traps along the Beaufort Sea shelf break during winter. *Can. J. Fish. Aquat. Sci.*, **49**, 663−670.

Frost, B.W. (1974) *Calanus marshallae*, a new species of calanoid copepod closely allied to the sibling species *C. finmarchicus* and *C. glacialis*. *Mar. Biol.*, **26**, 77−99.

Frost, B.W. (1989) A taxonomy of the marine calanoid copepod genus *Pseudocalanus*. *Can. J. Zool.*, **67**, 525−551.

Grebmeier, J.M. (2012) Shifting patterns of life in the Pacific Arctic and sub-Arctic Seas. *Annu. Rev. Mar. Sci.*, **4**, 63−78.

Grebmeier, J.M., Cooper, L.W., Feder, H.M. *et al.* (2006) Ecosystem dynamics of the Pacific-influenced northern Bering and Chukchi Seas in the Amerasian Arctic. *Prog. Oceanogr.*, **71**, 331–361.

Grønvik, S. and Hopkins, C.C.E. (1984) Ecological investigations of the zooplankton community of Balsfjorden, northern Norway: generation cycle, seasonal vertical distribution, and seasonal variations in body weight and carbon and nitrogen content of the copepod

Metridia longa (Lubbock). *J. Exp. Mar. Biol. Ecol.*, **80**, 93−107.

Hargrave, B.T., Bodungen B., Conover, R.J. *et al.* (1989) Seasonal changes in sedimentation of particulate matter and lipid content of zooplankton collected by sediment trap in the Arctic Ocean off Axel Heiberg Island. *Polar Biol.*, **9**, 467−475.

Hirche, H.-J. (1997) Life cycle of the copepod *Calanus hyperboreus* in the Greenland Sea. *Mar. Biol.*, **128**, 607−618.

Hirche, H.-J. and Kosobokova, K.N. (2011) Winter studies on zooplankton in Arctic seas: the Storfjord (Svalbard) and adjacent ice-covered Barents Sea. *Mar. Biol.*, **158**, 2359−2376.

Hirche, H.-J. and Niehoff, B. (1996) Reproduction of the Arctic copepods *Calanus hyperboreus* in the Greenland sea-field and laboratory observations. *Polar Biol.*, **16**, 209−219.

Hopcroft, R.R., Kosobokova, K.N. and Pinchuk, A.I. (2010) Zooplankton community patterns in the Chukchi Sea during summer 2004. *Deep-Sea Res. II*, **57**, 27−39.

Hunt, Jr.G.L. and Drinkwater, K. (2007) Introduction to the proceedings of the GLOBEC symposium on effects of climate variability on sub-Arctic marine ecosystems. *Deep-Sea Res. II*, **54**, 2453−2455.

Kaartvedt, S., Dale, T., Bagøien, E. *et al.* (2002) Bi-modal vertical distribution of the carnivorous copepod *Paraeuchaeta norvegica*. *J. Plankton Res.*, **24**, 155−158.

Knauer, G.A., Martin, J.H. and Bruland, K.W. (1979) Fluxes of particulate carbon, nitrogen, and phosphorus in the upper water column of the northeast Pacific. *Deep-Sea Res.*, **26A**, 97−108.

Kosobokova, K.N. and Hirche, H.-J. (2000) Zooplankton distribution across the Lomonosov Ridge, Arctic Ocean: species inventory, biomass and vertical structure. *Deep-Sea Res. I*, **47**, 2029−2060.

Kosobokova, K.N. and Hopcroft, R.R. (2010) Diversity and vertical distribution of mesozooplankton in the Arctic's Canada Basin. *Deep-Sea Res. II*, **57**, 96−110.

Makabe, R., Hattori, H., Sampei, M. *et al.* (2010) Regional and seasonal variability of zooplankton collected using sediment trap in the southeastern Beaufort Sea, Canadian Arctic. *Polar*

Biol., **33**, 257−270.

Markus, T., Stroeve, J.C. and Miller, J. (2009) Recent changes in Arctic sea ice melt onset, freezeup, and melt season length. *J. Geophys. Res.*, **114**, C12024. doi: 10.1029/2009JC005436.

Matsuno, K., Yamaguchi, A., Hirawake, T. *et al.* (2011) Year-to-year changes of the mesozooplankton community in the Chukchi Sea during summers of 1991, 1992 and 2007, 2008. *Polar Biol.*, **34**, 1349−1360.

Matsuno, K., Yamaguchi, A., Shimada, K. *et al.* (2012) Horizontal distribution of calanoid copepods in the western Arctic Ocean during the summer of 2008. *Polar Sci.*, **6**, 105−119.

McLaughlin, F., Carmack, E., Proshutinsky, A. *et al.* (2011) The rapid response of the Canada Basin to climate forcing: From bellwether to alarm bells. *Oceanography*, **24**, 146−159, http://dx.doi.org/10.5670/oceanog.2011.66.

Miller, C.B. (1988) *Neocalanus flemingeri*, a new species of calanidae (copepoda: calanoida) from the subarctic Pacific Ocean, with a comparative redescription of *Neocalanus plumchrus* (Marukawa) 1921. *Prog. Oceanogr.*, **20**, 223−273.

Miller, C.B. and Grigg, H. (1991) An experimental study of the resting phase in *Calanus finmarchicus* (Gunnerus). *Bull. Plankton Soc. Japan*, **special volume**, 479−493.

Miller, C.B., Cowles, T.J., Wiebe, P.H. *et al.* (1991) Phenology in *Calanus finmarchicus*; hypotheses about control mechanisms. *Mar. Ecol. Prog. Ser.*, **72**, 79−91.

Miller, C.B., Frost, B.W., Batchelder, H.P. *et al.* (1984) Life histories of large, grazing copepods in the subarctic ocean gyre: *Neocalanus plumchrus*, *Neocalanus cristatus* and *Eucalanus bungii* in the Northeast Pacific. *Prog. Oceanogr.*, **13**, 201–243.

Øresland, V. (1991) Feeding of the carnivorous copepod *Euchaeta antarctica* in Antarctic waters. *Mar. Ecol. Prog. Ser.*, **78**, 41–47.

Østvedt, O.J. (1955) Zooplankton investigations from weathership “M” in the Norwegian Sea, 1948−49. *Hvalrad. Skr.*, **40**, 1−93.

Ota, Y., Hattori, H., Makabe, R. *et al.* (2008) Seasonal changes in nauplii and adults of *Calanus hyperboreus* (Copepoda) captured in sediment trap, Amundsen Gulf, Canadian Arctic.

Polar Sci., **2**, 215−222.

Reynolds, R.W., Rayner, N.A., Smith, T.M. *et al.* (2002) An improved in situ and satellite SST analysis for climate. *J. Clim.*, **15**, 1609−1625.

Sampei, M., Sasaki, H., Hattori, H. *et al.* (2009) Significant contribution of passively sinking copepods to the downward export flux in Arctic waters. *Limnol. Oceanogr.*, **54**, 1894−1900.

Sampei, M., Sasaki, H., Forest, A. *et al.* (2012) A substantial export flux of particulate organic carbon linked to sinking dead copepods during winter 2007−2008 in the Amundsen Gulf (southeastern Beaufort Sea, Arctic Ocean). *Limnol. Oceanogr.*, **57**, 90−96.

Seiler, D. and Brandt, A. (1997) Seasonal occurrence of plankton Crustacea in sediment trap samples at three depth horizons in the Greenland Sea. *Polar Biol.*, **17**, 337−349.

Shimada, K., Carmack, E.C., Hatakeyama, K. *et al.* (2001) Varieties of shallow temperature maximum waters in the western Canadian Basin of the Arctic. *Geophys. Res. Lett.*, **28**, 3441−3444.

Shimada, K., Kamoshida, T., Itoh, M. *et al.* (2006) Pacific Ocean inflow: Influence on catastrophic reduction of sea ice cover in the Arctic Ocean. *Geophys. Res. Lett.*, **33**, L08605, doi: 10.1029/2005GL0256254.

Springer, A.M. and McRoy, C.P. (1993) The paradox of pelagic food webs in the northern Bering Sea-III. Patterns of primary production. *Cont. Shelf Res.*, **13**, 575−599.

Springer, A.M., McRoy, C.P. and Turco, K.R. (1989) The paradox of pelagic food web in the northern Bering Sea-II. Zooplankton communities. *Cont. Shelf Res.*, **9**, 359−386.

Stroeve, J., Holland, M.M., Meier, W. *et al.* (2007) Arctic sea ice decline: Faster than forecast. *Geophys. Res. Lett.*, **34**, L09501. doi: 10.1029/2007GL029703.

Sumata, H. and Shimada, K. (2007) Northward transport of Pacific summer water along the Northwind Ridge in the western Arctic Ocean. *J. Oceanogr.*, **63**, 363−378.

Tande, K.S. and Grønvik, S. (1983) Ecological investigations on the zooplankton community of Balsfjorden, northern Norway: sex ratio and gonad maturation cycle in the copepod

Metridia longa (Lubbock). *J. Exp. Mar. Biol. Ecol.*, **71**, 43−54.

Vinogradov, M.E. (1997) Some problems of vertical distribution of meso- macroplankton in the ocean. *Adv. Mar. Biol.*, **32**, 1−92.

Watanabe, E. and Ogi, M. (2013) How does Arctic summer wind modulate sea ice-ocean heat balance in the Canada Basin? *Geophys. Res. Lett.*, **40**, 1569−1574, doi:10.1002/grl.50363.

Watanabe, E., Kishi, M.J., Ishida, A. *et al.* (2012) Western Arctic primary productivity regulated by shelf-break warm eddies. *J. Oceanogr.*, **68,** 703−718, doi:10.1007/s10872-012-0128-6.

Weingartner, T., Aagaard, K., Woodgate, R. *et al.* (2005) Circulation on the north central Chukchi Sea shelf. *Deep-Sea Res. II*, **52**, 3150−3174.

Willis, K.J., Cottier, F.R., Kwaśniewski, S. *et al.* (2006) The influence of advection on zooplankton community composition in an Arctic fjord (Kongsfjorden, Svalbard). *J. Mar. Syst.*, **61**, 39−54.

Willis, K.J., Cottier, F.R., Kwaśniewski, S. (2008) Impact of warm advection on the winter zooplankton community in an Arctic fjord. *Polar Biol.*, **31**, 475−481.

Woodgate, R.A., Aagaard K., Swift, J.H. *et al.* (2005) Pacific ventilation of the Arctic Ocean's lower halocline by upwelling and diapycnal mixing over the continental margin. *Geophys. Res. Lett.*, **32**, L18609, doi: 10.1029/2005GL023999.

Woodgate, R.A., Weingartner, T. and Lindsay, R. (2010) The 2007 Bering Strait oceanic heat flux and anomalous Arctic sea-ice retreat. *Geophys. Res. Lett.*, **37**, L01602. doi: 10.1029/2009GL041621.

Yamaguchi, A. and Ikeda, T. (2000) Vertical distribution, life cycle, and body allometry of two oceanic calanoid copepods (*Pleuromamma scutullata* and *Heterorhabdus tanneri*) in the Oyashio region, western North Pacific Ocean. *J. Plankton Res.*, **22**, 29−46.

Yamaguchi, A. and Ikeda, T. (2001) Abundance and population structure of three mesopelagic *Paraeuchaeta* species (Copepoda: Calanoida) in the Oyashio region, western subarctic Pacific Ocean with notes on their carcasses and epizonic ciliates. *Plankton Biol. Ecol.*, **48**, 104−113.

Figure legends

Fig. 1. Location of St. NAPt (Northwind Abyssal Plain trap) in the western Arctic Ocean where the sediment trap was moored at 184 m during October 2010 to September 2011. ACW: Alaskan Coastal Water, AW: Anadyr Water, BSW: Bering Shelf Water.

Fig. 2. Seasonal changes in depth (a) and temperature (b) monitored for shallower trap at St. NAPt during October 2010 to September 2011. Current velocity at 45 m and 188 m of St. NAPt (c) estimated by a physical ocean general circulation model: Center for Climate System Research Ocean Component Model (COCO) version 4.9. Temperature (d) and salinity (e) observed from CTD casts at St. NAPt in 30 October 2010 and 21 September 2012. Shades indicate the trap depths (180−190 m). SML: Surface Mixed Layer (0−25 m), PSW: Pacific Summer Water (25−100 m), PWW: Pacific Winter Water (100−250 m), AW: Atlantic Water (>250 m).

Fig. 3. Seasonal changes in sea ice concentration for the investigation area during the sampling period (http://iridl.ldeo.columbia.edu/SOURCES/.IGOSS/.nmc/.Reyn_SmithOIv2/, data from Reynolds *et al.*, 2002), total mass flux (<1 mm size fraction) collected by sediment trap, surface chl. *a* from satellite (a) and daylight hours (b) at St. NAPt during 4 October 2010 to 28 September 2011.

Fig. 4. Results of cluster analysis based on the flux of zooplankton swimmers. Twenty six samples were clustered into three groups from Bray-Curtis dissimilarity (a). Seasonal changes in zooplankton swimmer flux, species composition and clustered groups collected by sediment trap moored at 184 m of St. NAPt during 4 October 2010 to 28 September 2011 (b).

Fig. 5. Seasonal changes in flux and copepodid stage composition of the four dominant copepods: *Calanus hyperboreus* (a), *Metridia longa* (b), *Paraeuchaeta glacialis* (c), *Heterorhabdus norvegicus* (d), at 184 m of St. NAPt during 4 October 2010 to 28 September 2011.

Fig. 6. Seasonal changes in flux, lipid accumulation (upper panels) and gonad maturation (lower panels) compositions (stage I−III) of C6Fs of *Calanus hyperboreus* (whole n = 232) (a, d),

Metridia longa (*n* = 234) (b, e) and *Paraeuchaeta glacialis* (*n* = 166) (c, f) at 184 m of St. NAPt during 4 October 2010 to 28 September 2011. *: Egg sac attached individual was occurred.

Fig. 7. Seasonal changes in flux and lipid accumulation composition (I−III) of the Pacific *Neocalanus cristatus* C5 collected by sediment trap moored at 184 m of St. NAPt during 4 October 2010 to 28 September 2011.

Fig. 8. Schematic diagram on seasonal changes in daylight hours, sea ice concentration, chl. *a*, total mass flux (upper panel), swimmer community, population structure and reproduction period of copepods (*C. hyperboreus*, *M. longa*, *P. glacialis* and *H. norvegicus*), and occurrences of the Pacific *N. cristatus* collected by sediment trap at 184 m of St. NAPt during 4 October 2010 to 28 September 2011 (lower panel). For *C. hyperboreus*, *M. longa* and *P. glacialis*, reproduction period was evaluated by C6F gonad maturation (Fig. 6d−f). For *H. norvegicus*, their reproduction period was estimated by the occurrence of early copepodid stages (Fig. 5d).

Table 1. Comparison of zooplankton swimmer community collected by sediment trap in the Arctic Ocean.

Region (position)	Period	Depth (m)	Dominant taxa/species (percentage to total zooplankton flux in number)	References
Amundsen Gulf (71°47´N, 126°30´W)	Oct. 2007–July 2008	112	*M. longa* (50), *P. glacialis* (6), *C. hyperboreus* (2), *C. glacialis* (2)	Sampei *et al.* (2012)
Amundsen Gulf (70–72°N, 123–135°W)	Oct. 2003–Aug. 2004	100, 200, 400	*Oncaea* spp. (34), *M. longa* (21), pteropods (11), *C. hyperboreus* (4)	Makabe *et al.* (2010)
Beaufort Sea Shelfbreak (69–72°N, 127–139°W)	Sep. 1987–Mar. 1988	115, 128, 145	*M. longa* (49), amphipods (27), *P. glacialis* (15), *C. hyperboreus* (8)	Forbes *et al.* (1992)
East Greenland Sea (72°0´–30´N, 7°2´–43´W)	July 1989–July 1992	500	*M. longa* (59), *H. norvegicus* (12), amphipods (9), ostracods (8)	Seiler and Brandt (1997)
Kongsfjorden (79°1.2´N, 11°46.4´E)	Sep. 2005–May 2006	115	*C. finmarchicus*, *C. glacialis*, *M. longa*, *P. norvegica*	Willis *et al.* (2008)
Kongsfjorden (79°3.2´N, 11°18.0´E)	Apr.–June, July–Sep. 2002	215	*C. finmarchicus*, *C. glacialis*, *C. hyperboreus*, *P. norvegica*	Willis *et al.* (2006)
Axel Heiberg Island (81°N, 96–98°W)	Sep. 1986–June 1987	100	*C. hyperboreus* (78), *M. longa* (9), *P. norvegica* (4), *C. glacialis* (2)	Hargrave *et al.* (1989)
Northwind Abbysal Plain (75°47´N, 126°30´W)	Oct. 2010–Sep. 2011	180	*H. norvegicus* (17), *M. longa* (16), *P. glacialis* (15), *C. hyperbpreus* (8)	This study

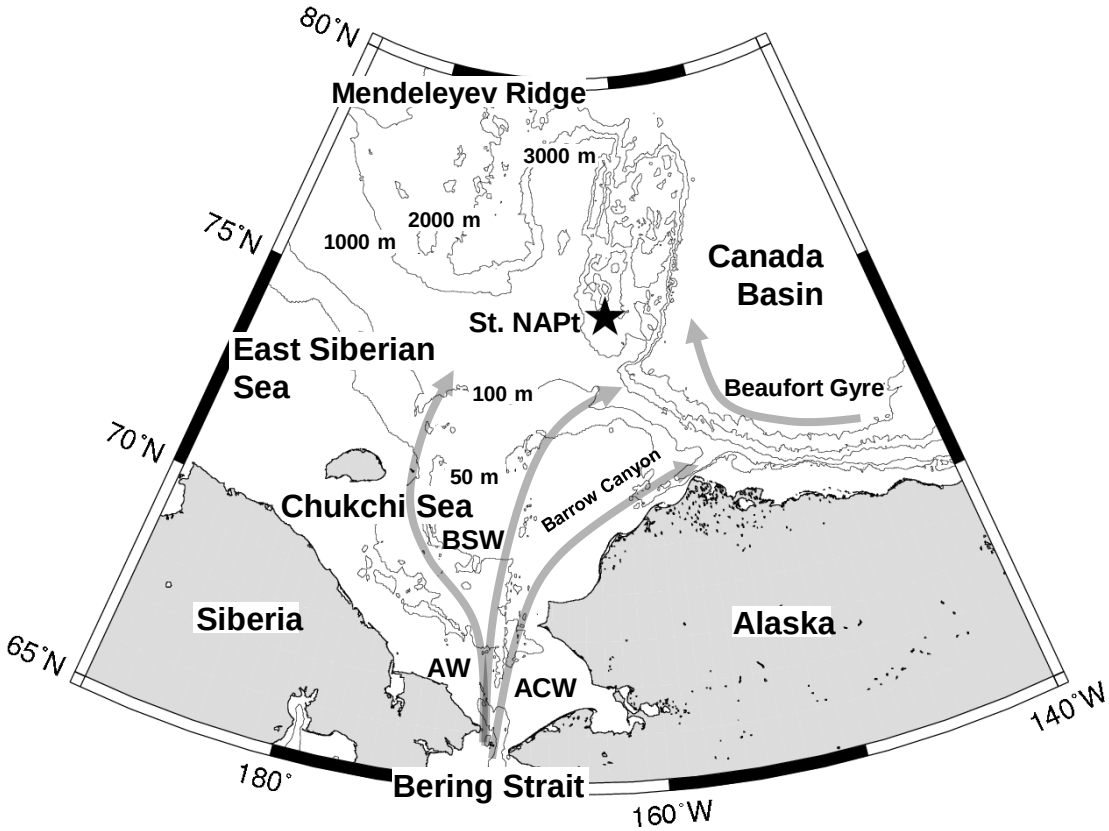

Fig. 1 (Matsuno et al.)

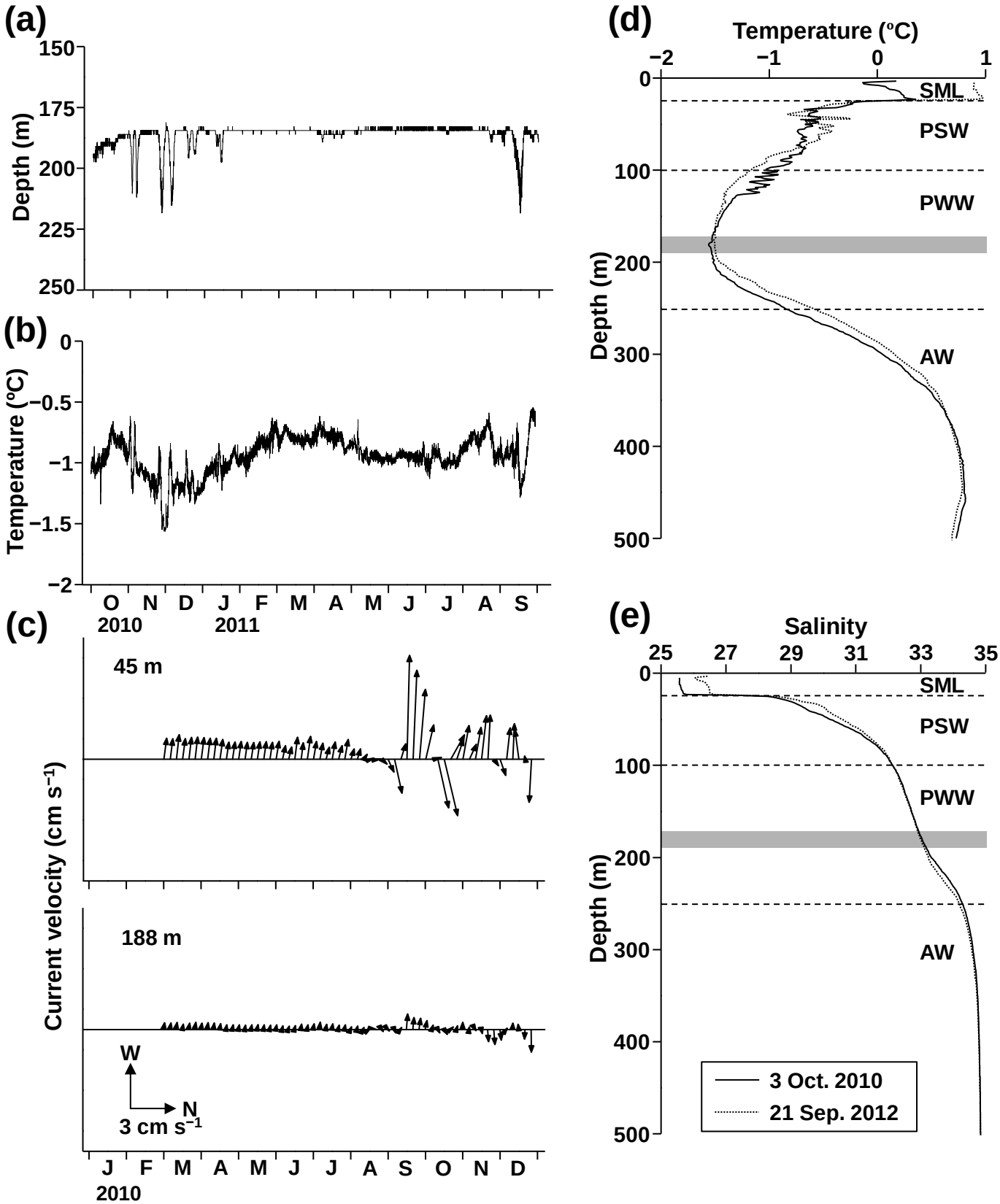

Fig. 2 (Matsuno et al.)

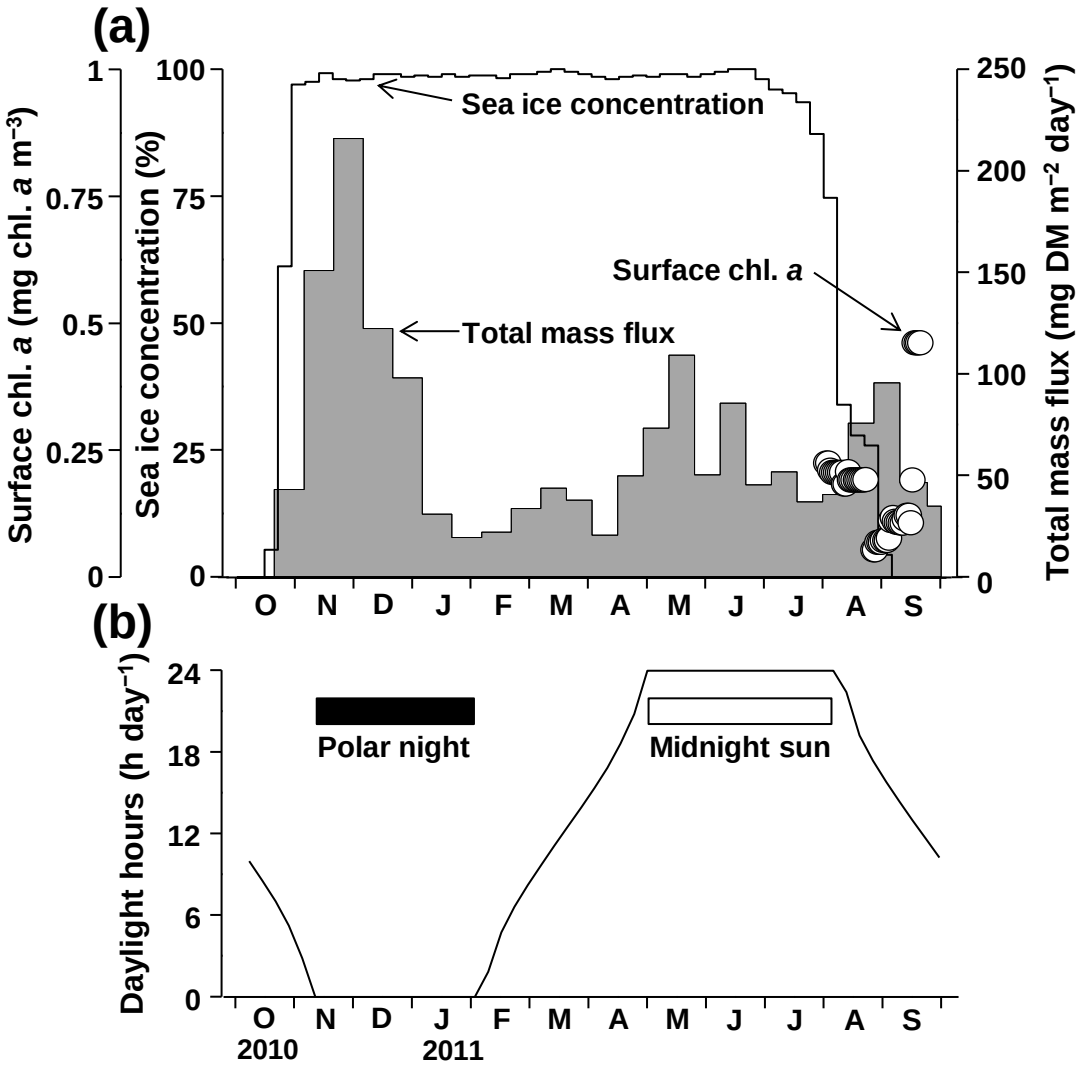

Fig. 3 (Matsuno et al.)

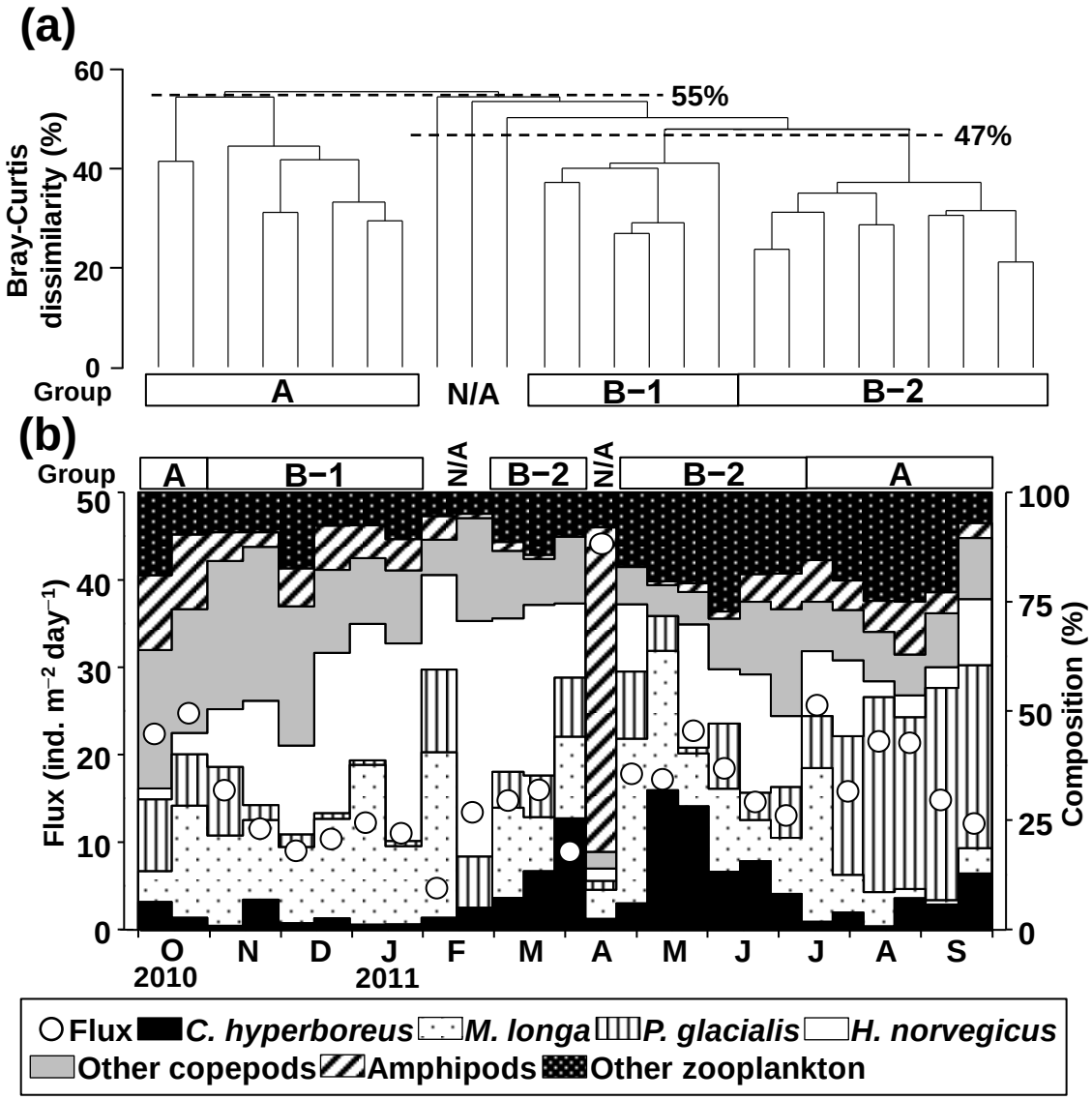

Fig. 4 (Matsuno et al.)

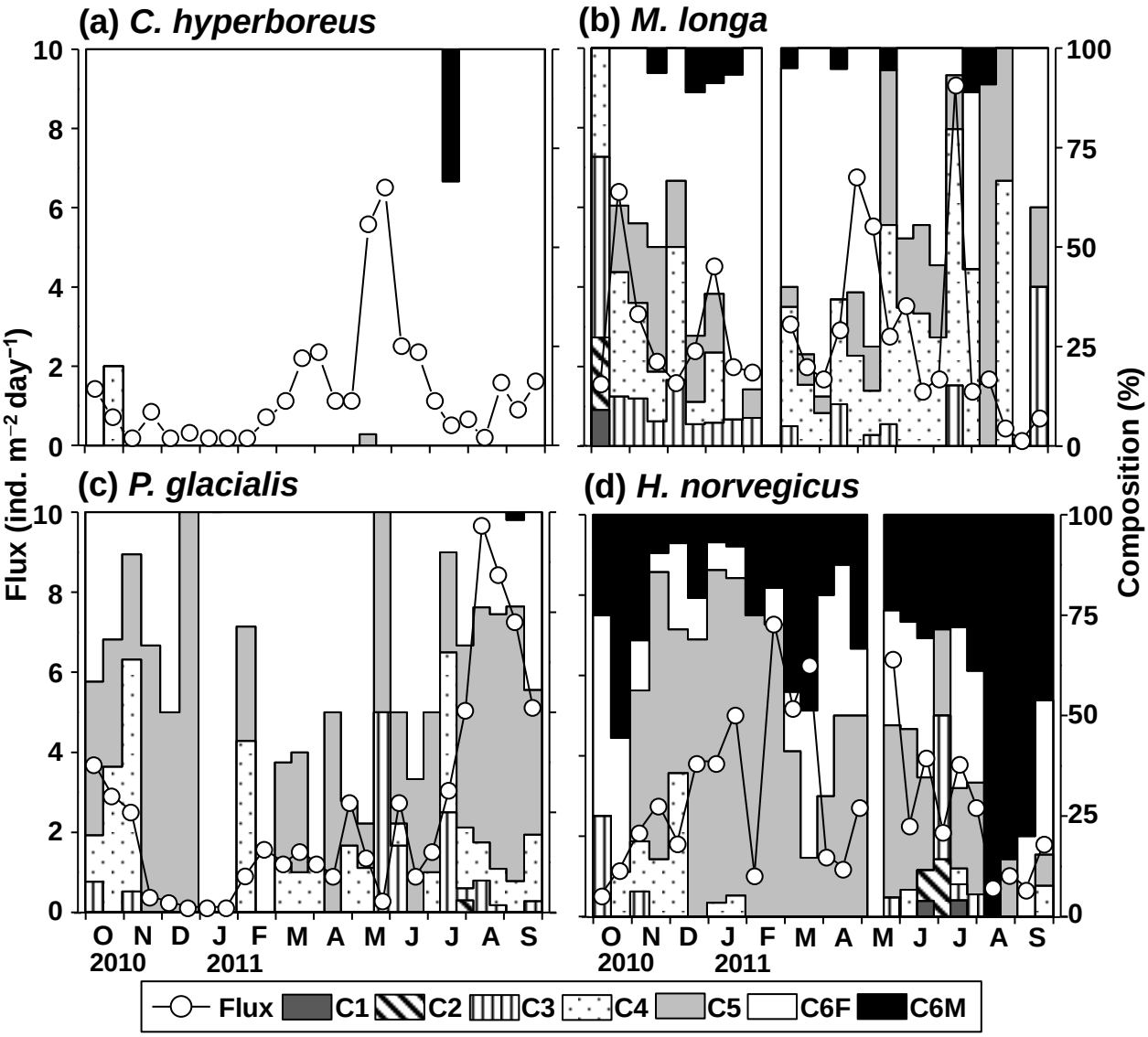

Fig. 5 (Matsuno et al.)

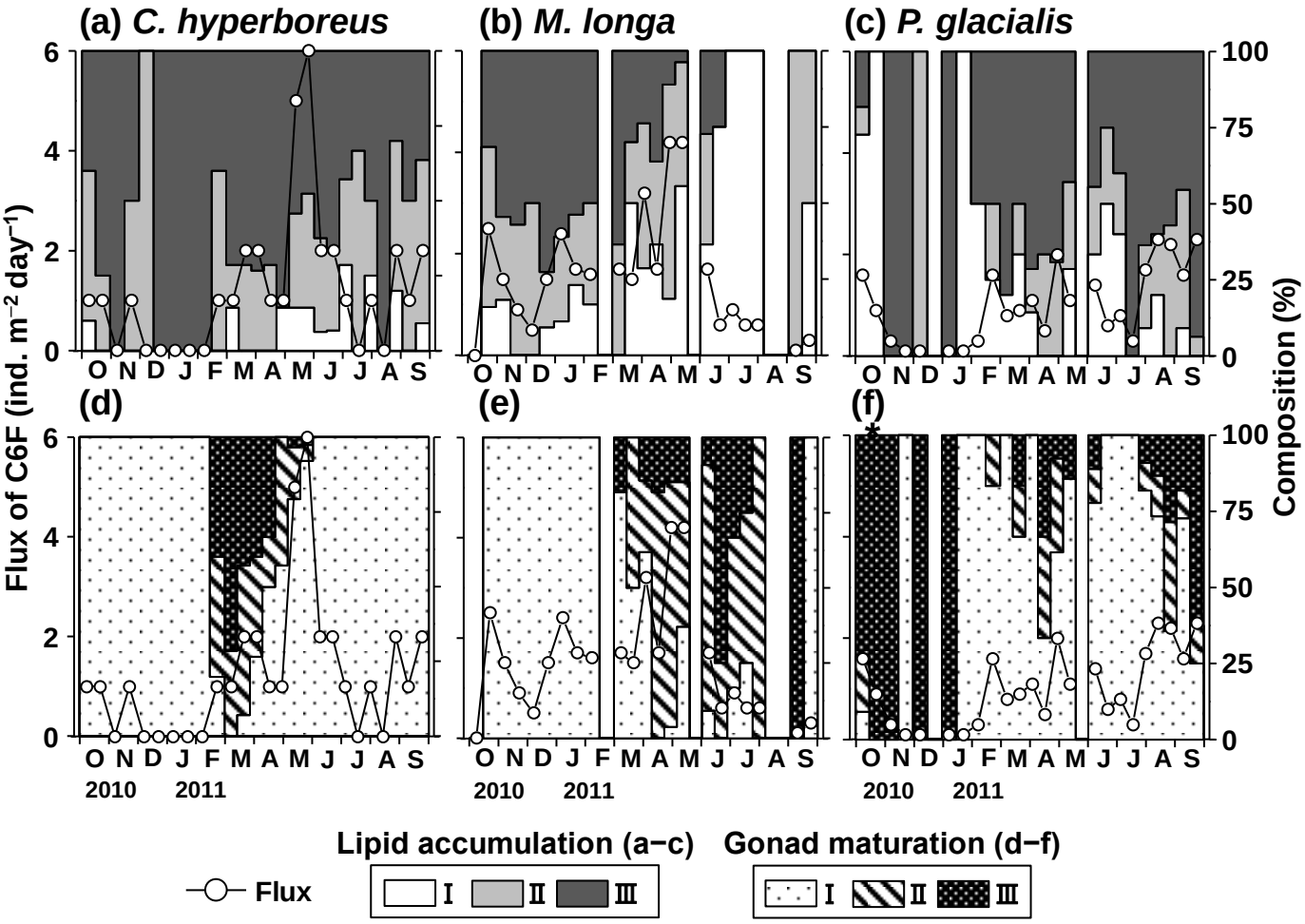

Fig. 6 (Matsuno et al.)

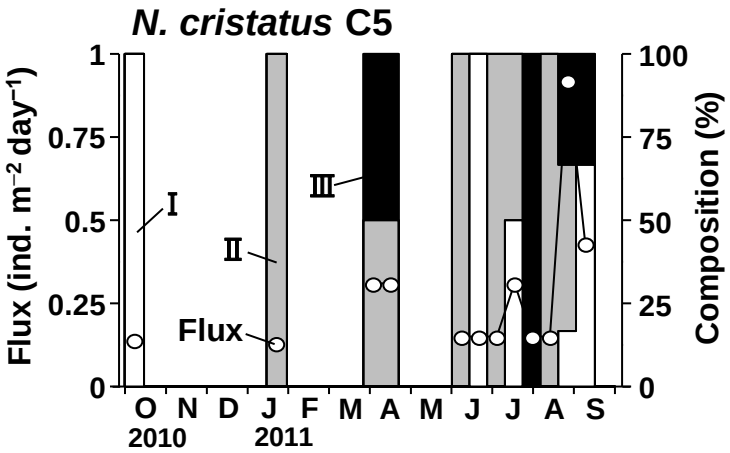

Fig. 7 (Matsuno et al.)

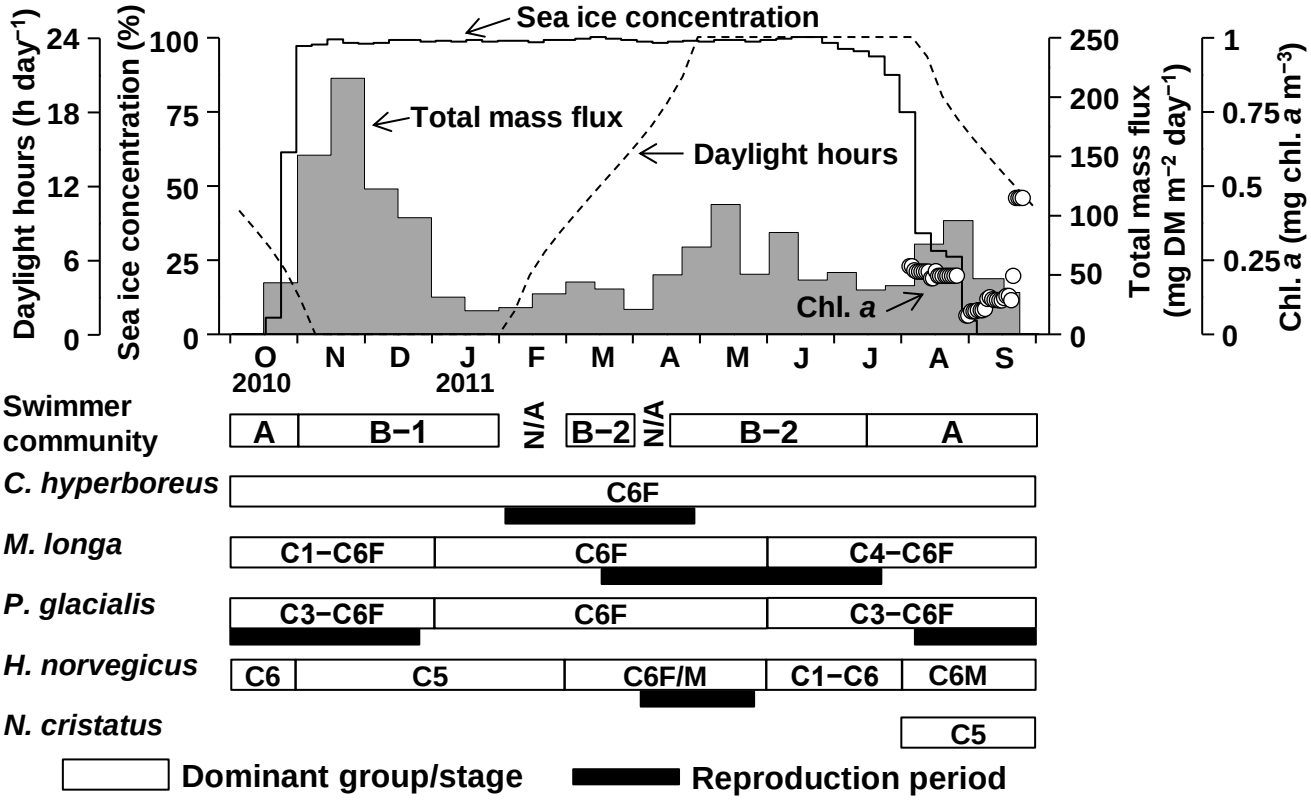

Fig. 8 (Matsuno et al.)